## **VUDURU M.A.E. Jemison Crewed Ascent Vehicle (JCAV)**



Villanova University (VU), Drexel University (DU), Rutgers University (RU)

May 27th, 2021

Nicholas Florio - VU, EE - Graduate Henri Doucet - VU, ME Sanskar Agrawal - VU, EE Jonathan Rodriguez - VU, Astro Samuel Gunther - VU, Astro Joseph Krueger - VU, ME Adam Hine, VU, EE Michael Blandino - VU, ME Anupam Mishra - DU, ME
Joe Fasso - DU, EE
Lauren Hall - DU, ME
Kate Hazaveh - DU, SE
Brandon Buell - DU, ME
Max Millenbach - DU, ME
Srivatsa Ganesh - DU, ME
Jason Walat- DU, ME
Munazzah Al Hashim- Du, ME

Devin Lewis - RU, AE
Christopher Eden - RU, AE
Taha Kaleem - RU, Physics
Siddharth Sambath Ramkumar - RU, AE
David Samolkin - RU, AE
Brian McNicholas - RU, ME

Advisors: Dr. Sergey Nersesov (VU), Dr. Sridhar Santhanam (VU), Mike Simard (VU), Lars Osborne (Agile Space Industries), Prashanth Bangalore (Agile Space Industries), Michael Staab (Northrop Grumman)

Credit to Emily Dupervill (Villanova) & Juan Cortes (Carnegie Mellon) for Logo Artwork

(Team members all undergraduates unless listed)

### Table of Contents & Figures

#### I. Abbreviation List

#### II. Introduction

- A. Mission Profile Definition
- B. Mission Architecture

Figure 1: Mission CONOPS

C. Design Requirements

## III. Launch Trajectory

## IV. Orbital Transfers & Delta-V Budget

Figure 2: Map of Orbital Trajectory

## V. Environmental Conditions

Figure 3: Path to Launch Site

Figure 4: Path Incline

Figure 5: NE Syrtis region in Winter

Figure 6: Temperature Data for ~20°N

Figure 7: Mars Global Climate Zones

Figure 8: Dust Correction Factor

Figure 9: Daytime & Nighttime Temperatures throughout year

Table 1: Dates of Significance

## VI. Mass Estimate

Table 2: Subsystem and Associated Mass

Figure 10: FEA Landing Legs

Figure 11: FEA Tank Mount

## VII. MAV Design

Figure 12: Landed Configuration

Figure 13: Orbital Configuration

Figure 14: Dimension Views of top and side of JCAV

Figure 15: View of sample storage system

## VIII. Engine Configuration

Table 3: Summary of chemical propulsion system parameters

Table 4: MAVE specifications from RPA

Table 5: MAVE dimensions from RPA

Figure 16: MAVE CAD model & RPA design schematic

Figure 17: Top view of MAVE

Figure 18: Side View of MAVE

## **IX.** Propellant Selection

Table 6: Propellant tank design summary

#### X. Thermal Information

Table 7: MLI Insulation heat flux temperature differences

Figure 19: Dimensions of heater configuration

## XI. Human Factors

## XII. Power, Avionics, & Communications (PAC) Systems

Figure 20: JCAV Power Budget

Figure 21: Communications Map

## XIII. Development Timeline and Cost Estimate

Table 8: Total Mission Cost Estimates

Table 9: Budget Breakdown

Figure 22: Development timeline

## XIV. Risk Analysis & TRL

Table 10: Risk Analysis Matrix

Table 11: Technology readiness Levels

## XV. Quad Chart

## XVI. Appendix

- A. Calculations
- B. References

#### **Abbreviation List:**

ΔV - Delta-V

AACE - Association for the Advancement of Cost Engineering

CDR - Critical Design Review

DSN - Deep Space Network

ECLSS - Environment Control and Life Support System

ERV - Earth Return Vehicle

EVA - Extravehicular Activity

FEA - Finite Element Analysis

FRR - Flight Readiness Review

ISRU - In-Situ Resource Utilization

IVA - Intra Vehicular Activity

JCAV - Jemison Crewed Ascent Vehicle

JMARS - Java Mission-Planning and Analysis for Remote Sensing

LMO - Low Mars Orbit

MAV - Mars Ascent Vehicle

MAVE - Mars Ascent Vehicle Engine

MECO - Main engine Cut-Off

MEMLI - Multi-Environment Multi-Layered Insulation

MMH - Monomethylhydrazine

MON25 - mixed oxide of nitrogen containing 25 % nitric oxide (NO) with the balance being nitrogen tetroxide (NTO, N2O4)

MPS - Main Propulsion System

ORR - Operational Readiness Review

PMDBU - Power & Management Diversified Bus Unit

PDR - Preliminary Design Review

RCS - Reaction Control System (utilized as orbit course and angle thruster)

RPA - Rocket Propulsion Analysis

SDR - System Definition Review

SECO - Second-stage Engine Cut-Off

SLS - Space Launch System

SSTO - Single Stage to Orbit

TRL - Technology Readiness Level

VUDURU - Villanova University, Drexel University, and Rutgers University

#### Introduction:

#### **Mission Profile Definition**

With a growing interest in crewed missions to Mars, the space industry has realized several challenges in achieving such a feat. One of the largest obstacles is reducing the size of the Mars Ascent Vehicle (MAV), which will be tasked with transporting a crew from the surface of Mars to low Mars orbit. The VUDURU Mars Ascent Expedition (MAE) team addresses such a challenge with their Jemison Crewed Ascent Vehicle (JCAV). As one can observe, the team has embarked upon honoring the first African American female astronaut, Mae C. Jemison. Just as Mae has trail-blazed and inspired so many, the team hopes to do the same with their innovative, robust, minimal MAV design fully capable of advancing exploration of Mars.

#### **Mission Architecture**

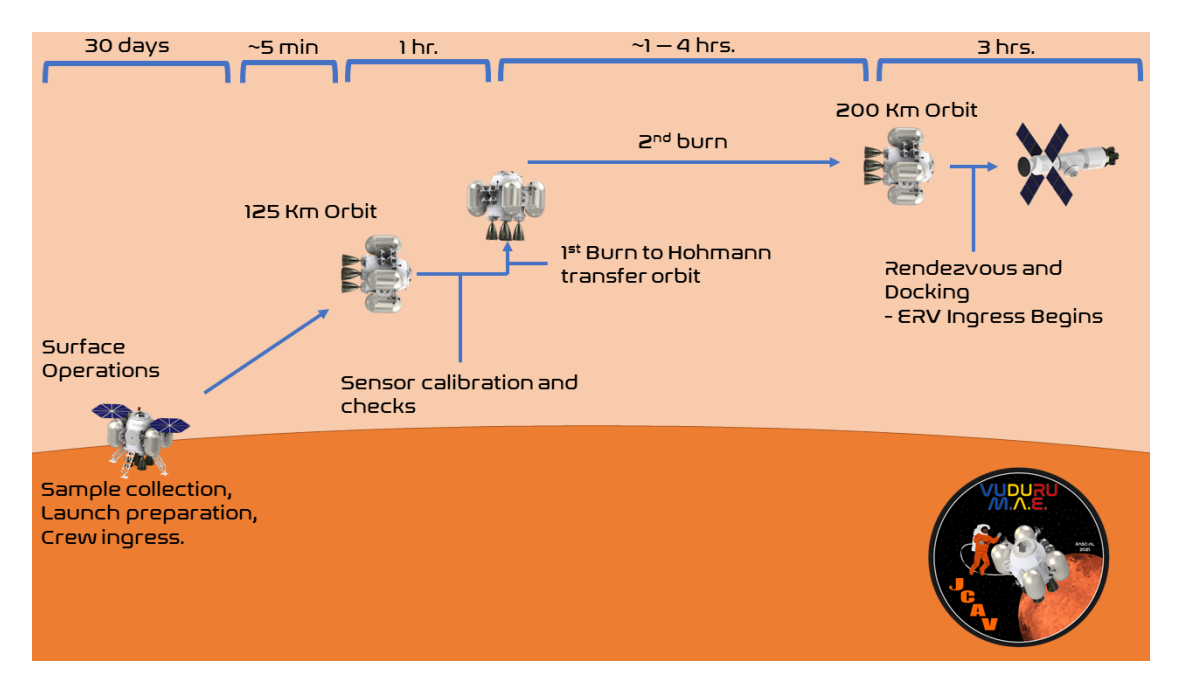


Figure 1: Mission CONOPS

#### **Design Requirements:**

The Jemison Crewed Ascent Vehicle (JCAV) is constrained by and meets the following design requirements:

- Delivers a crew of 2 from Mars surface to ERV: Life support system capable of handing the crew for at least 2 days (with an expected 5.6 hour journey, and an assumed maximum of 9.7 hours for a missed orbit)
- 5,000kg dry mass limit || 20,000kg wet mass limit: MAV has a total estimated mass (accomadating 400 kg of samples) of 19136 kg, with a dry mass of 4136 kg, and 15000 kg of fuel.
- Necessary support interfaces: JCAV requires a Mars rover capable of docking with JCAV's ingress tube, an Earth return vehicle (ERV) in a 200 km orbit, a Mars orbiter for relay communications, and an available SLS block 1B for launching to Mars.
- Tech and System Development Timelines realistically serve mission landing date by 12/31/2034: development and manufacturing of JCAV requires the use of innovative technology solutions, including the development of a MON-25 and MMH main engine by Agile,

- multi-environment multi-layer tank insulation, rotating sample storage system, and minimum ingress tunnel concept, all estimated to be integrated and tested by April 2033.
- **Budget of no more than \$2 billion yearly from 2025-2035:** *The MAV is budgeted for a total of \$11.8 billion and is under the \$2 billion maximum for each year.*
- **Mission Duration:** The JCAV mission is estimated to be ready for launch by April 11, 2033, arriving in Martian orbit on December 26, 2033.

#### **Launch Trajectory**

The Mars Ascent Vehicle will be launched from a launch site near NE Syrtis at an orbital inclination of 18.154° and launch azimuth of 90°. This will allow for the MAV to launch parallel to the equator. The Earth Return Vehicle (ERV) will be in a 200 km orbit in the same orbital plane as the MAV. The MAV will gain altitude until reaching an altitude of 125 km, 45 km above the Martian Karman line at which point it will enter initial orbit. Due to Mars having a low atmospheric density, the effects of drag as it ascends will be nearly negligible, particularly above the Karman line.

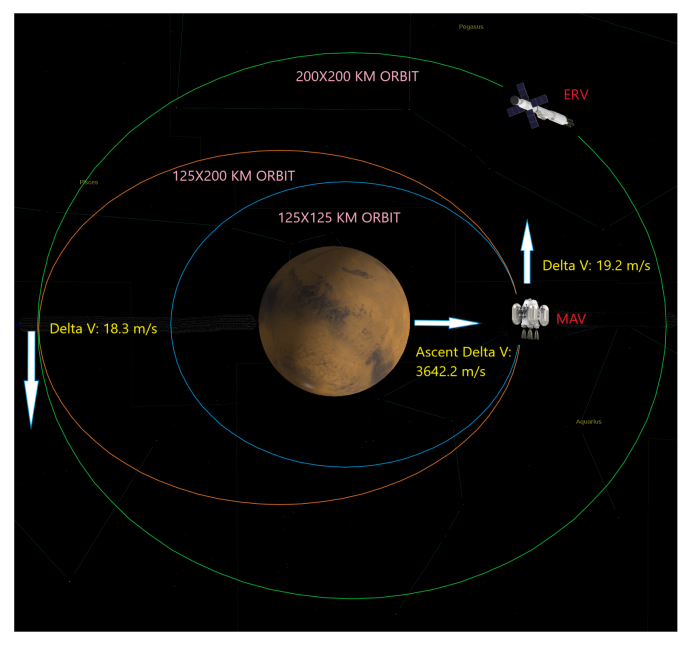
For the MAV to successfully dock with the ERV, it is recommended that the MAV launches when the ERV has a true anomaly of 14.1 degrees from the apse line, with an argument of periapsis of 90 degrees. When the MAV launches, it will go through a single stage to orbit. For this single stage launch to complete, it will take a total burn time of around 480.78s, with a max gravitational force of 2.17 g. The delta-V for the launch of the MAV to an altitude of 125 km is determined to be 3489.7 m/s, however, the MAV experiences a gravity loss of 480.04 m/s as its altitude increases and Mars rotation has a benefit of 159.25 m/s on the launch. This results in the total delta-V for launch being 3810.49 m/s.

#### **Orbital Transfers & Delta-V Budget**

After the MAV reaches its initial 125 km circular orbit, it will stay there in a parking orbit until there is confirmation on whether or not it can do its second burn to go into the Hohmann transfer orbit. Doing so ultimately allows for the transition into the 200 km circular orbit to dock with the ERV. The orbit of the ERV was changed from a 250km x 1 sol to a 200 km x 200 km orbit. This was changed since this will reduce the risk associated with failure to dock on the MAV's first attempt, as it will have a period of only 1.82 hr and its altitude will be high enough to not require excessive burning of propellant to remain in orbit. Additionally, this will significantly help in decreasing the total time it takes for the MAV to reach the ERV. The initial parking orbit was also changed from 100 km to 125 km orbit to ensure there are no drag effects on the MAV. The effects of drag at 125 km should be minimal as suggested in the paper *Optimization of the Mars Ascent Vehicle for Human Space Exploration*, which describes that the effects of drag on the thrust are analyzed for a 100 km parking orbit and are shown to affect the delta-V by 18 m/s [1]. In this article, this was shown to be negligible and not of concern. Therefore, for a 125 km orbit, drag would surely not be of concern. If necessary, to compensate for the effects of drag on the vehicle, the MAV may use extra fuel to do slight burns, which will ensure that the MAV matches the orbital speed.

While in the 125 km orbit, the MAV will complete one orbit every 1.76 hours and will keep a constant speed of about 3489.72 m/s. In this planned mission, the MAV will first complete one orbit around Mars, during which the crew will do sensor calibrations and perform checks to make sure everything in the MAV is working properly. As the MAV approaches the zero degree line at the horizontal, the ERV should be at an angle of 2.79 degrees with respect to the MAV. At this moment, the MAV will do its first orbital burn to enter the Hohmann transfer orbit of 125 km x 200 km, which has an orbital period of 1.789 hours. This burn will require a delta-V of 19.2 m/s [2]. If all the launch times have gone successfully, the MAV will then remain in this orbit until the ERV approaches its periapsis and successful docking is foreseeable. At this point, the second orbital burn will be performed at the apoapsis of the transfer orbit, which will have a delta-V of 18.283 m/s [2], so that the MAV can enter into the 200 km orbit, leading slightly ahead of the ERV. At this point, since the ERV and the MAV will have matching speeds and trajectories, the MAV can then proceed to go through the process of rendezvous and docking. After consulting with

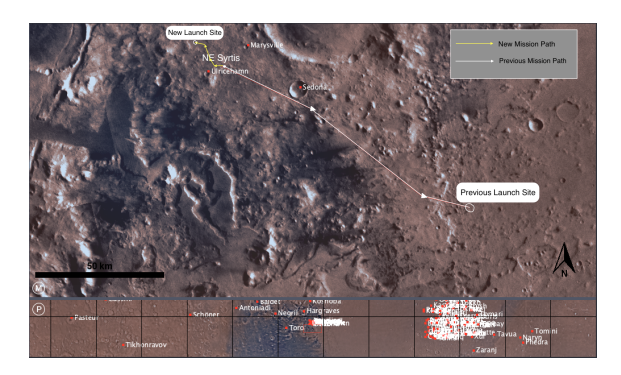
several NASA engineers, we were able to conclude that we can estimate the docking and rendezvous to be around three hours. If by any case the ERV docking is not successful, the MAV will remain in the 125 x 200 km transfer orbit until the ERV completes a 200 km orbit and comes in proximity with Mars again. Through simulations in MATLAB and Excel, we were able to determine the timings for a second attempt and a third attempt. Performing a second attempt would take an additional 1.7179 hours and to do yet another attempt would take an additional 2.33 hours. Therefore, with these numbers the total flight time for the first attempt at docking with the ERV would be 5.644 hours. then for a second attempt 7.3619 hours and lastly, for a third attempt, around 9.701 hours. If everything goes well on the first attempt, then the total delta-V for meeting up with the ERV would be 3791.94 m/s, which is calculated with



the benefit of the rotation of Mars on the Figure 2: Orbital Trajectory (Made using GMAT and 3D Paint tools) trajectory which is around 56.38 m/s. This required delta -v is significantly less than the total delta-v that the MAV has available, therefore, there is roughly 1300 m/s, which includes 197.80 m/s of RCS thrusters, of extra delta v that the MAV can use for further attempts, docking and for course adjustments.

#### **Environmental Conditions**

The VUDURU MAE Jemison Crewed Ascent Vehicle (JCAV), is proposing to land at18 N,77 E, known as the NE Syrtis site. These coordinates are located in the Utopia Planitia region of Mars, which has been proposed as a potential exploration zone for human missions to the surface of Mars [3]. The humans will travel to18.154 N, 76.82 E, which is the launch site that is 16.76 km away from the NE Syrtis site according to the generalized path created in Figure 6. The team previously proposed to launch at a location that was 112.73 km away from NE Syrtis site because it was believed to have been the only other safe, flat region to launch from. This previous location would have also included a total incline of 1,773 km. The new coordinates were chosen in an effort to conserve energy, reduce travel time, and increase the efficiency of the mission.



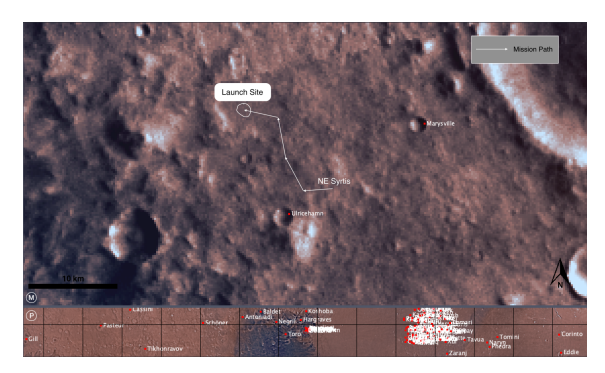


Figure 3

The left image was taken from the JMARS [4] software. The path begins at coordinates  $18.154^{\circ}N$ ,  $76.82^{\circ}E$  and ends at the coordinates  $18^{\circ}N$ ,  $77^{\circ}E$ , which is by the Ulricehamn landmark. The right image is zoomed in further.

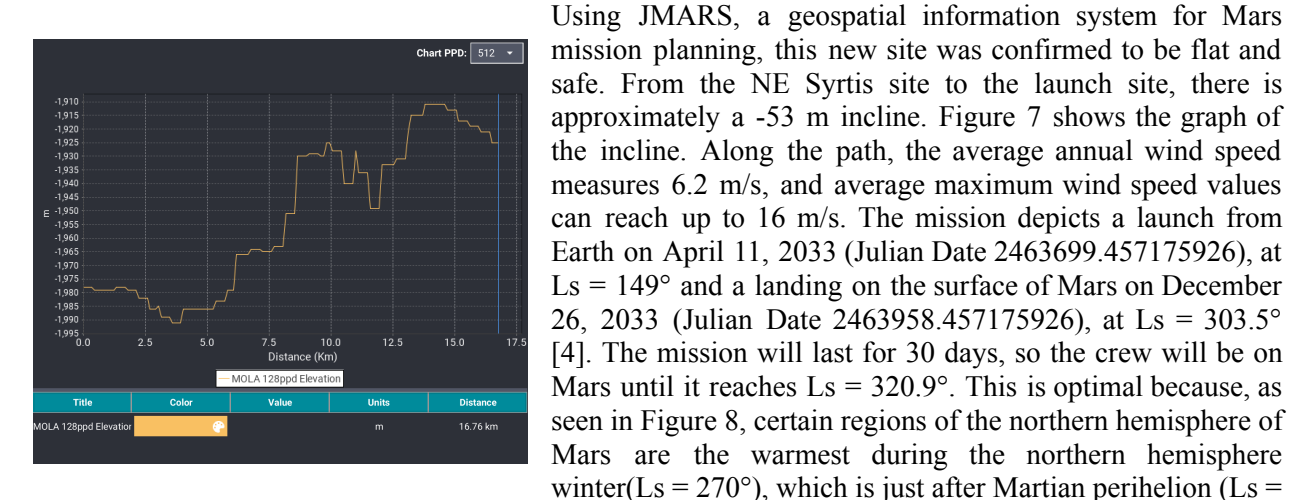
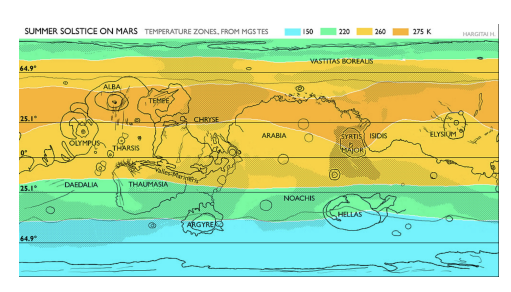


Figure 4  $$260^{\circ}$) [3].$  The incline from the launch site to NE Syrtis in meters.



MATTON FORMULE

WATTON FORMULE

AAABA

ATTON MATTON FORMULE

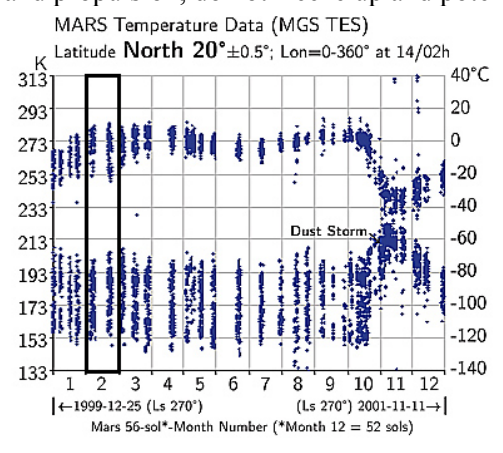
WATTON FORMULE

W

Figure 5

The NE Syrtis region is warmer during the northern hemisphere winter.

Using the data shown in Figure 9, temperature stability around month eleven due to dust storms can be observed. This data bolsters the decision of landing during winter as it is also the end of dust storm season on Mars [5]. Operating during the warmest part of the year ensures that systems on board, such as power and propulsion, do not freeze up and potentially cause damage to onboard hardware. While at the NE



Syrtis site, the humans will be experiencing some of the lowest albedo values in the region, meaning surface temperatures will be higher on average [6] compared to other regions. Figure 10 shows the Martian climate zones, which demonstrates the albedo levels on the entire Martian surface [7]. The north and south poles of Mars have high albedo, meaning they reflect a larger relative portion of sunlight, whereas the NE Syrtis region has a relatively low albedo. One potential risk posed to the astronauts is the fact that global Martian dust storms begin just after perihelion, however it appears they will be arriving after the peak intensity of the storms [8].

Figure 6

This image depicts temperature data for ~20 °N.

Dust accumulation poses minimal risk as it can grow to only a few micrometers in thickness, which the humans can remove with sensitive dust removal rags, compressed air, or a vacuum [9]. The dust storms

mainly affect the amount of solar radiation being received, which can be seen in Figure 11. At approximately an Ls of 303°, the Curiosity rover measured a 17% decrease of solar flux on Martian year (MY 32) and a 10% decrease on MY 33. Figure 12 shows the temperatures on Mars over different latitudes throughout the year for both daytime and nighttime.

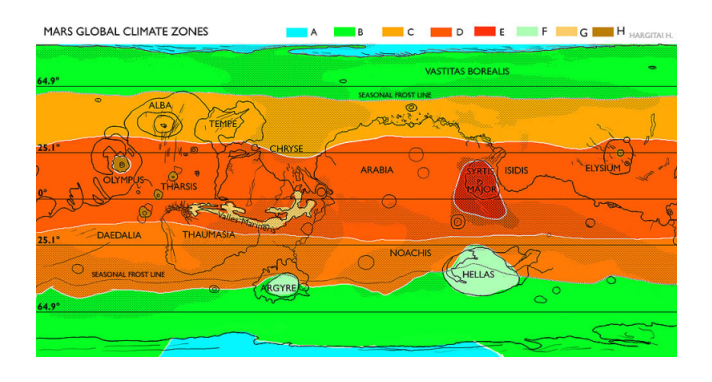
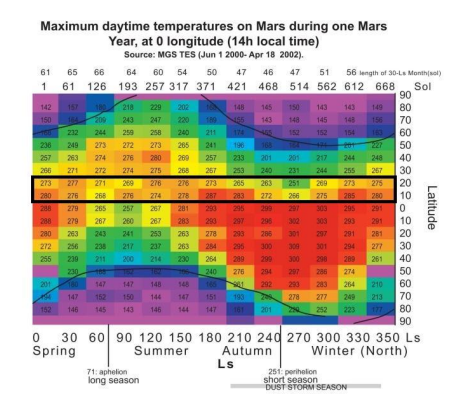


Figure 7
This image depicts Mars Global Climate Zones based off of albedo as well as other variables. [5]



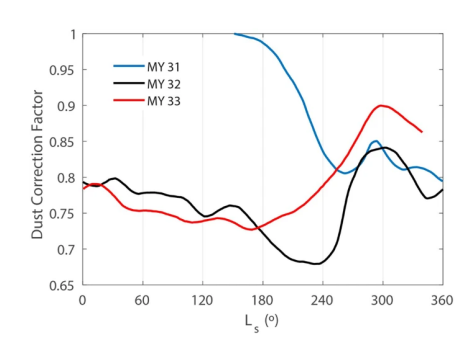


Figure 8
The Dust Correction Factor is a measure of (normalized) solar flux that the Curiosity rover receives.

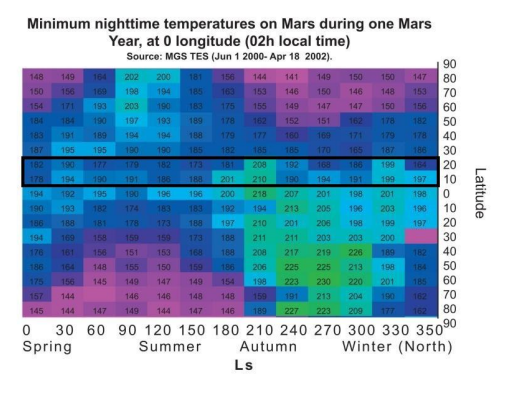


Figure 9: The left image is a map of daytime temperatures on Mars throughout the year over different latitudes. The right image shows nighttime temperatures for the same latitudes.

	Date	Julian Date	Solar Longitude (Ls)	Martian Month
Launch Date (from Earth)	April 11, 2033	2463699.457175926	149°	5
Arrival Date (on Mars)	December 26, 2033	2463958.457175926	303.5°	11
Launch Date (from Mars)	January 25, 2034	2463988.457175926	320.9°	11

Table 1.

These are the dates of significance, along with their respective Julian Date, Solar Longitude, and Martian Month.

#### **Mass Estimate**

Subsystem	Mass (kg)
Crew Cabin and Structures	1,368
Ingress Tunnel	120
Communications	103
Avionics	30
Electronics and Power	735
ECLSS	223
MPS and Empty Tanks	1,199
Crew (2)	197
1.5 Days of Oxygen and O2 (and tanks)	30
IVA suits (2)	31
Samples	100
Dry Mass total	4,136
Propellent	15,000
Fueled MAV total	19,136

Table 2.: Subsystems and their Masses

Mass of the MAV is one of the driving constraints for this design. Given the 5000 kg dry mass limit and 15,000 kg fuel limit (with a total limit of 20,000 kg), tracking the masses of the various subsystems was critical to meet design requirements. As of the current design of the JCAV, the total dry mass of 4,136 kg provides design with a 17% mass margin on components.

In order to optimize mass, FEA was conducted on team-designed structural components. Specifically, the landing legs and tank mounts (assumed to be aluminum), which are both mission critical and large sources of structural mass. Structural analysis was conducted by applying the maximum load to components: the landing legs were tested under 5000 kg and the tank mounts under the total propellant mass of 15,000 kg. Masses were reduced on these components while still maintaining a safety factor of 2. This method allowed for mass savings upwards of 500 kg, allowing for more components to be added to other subsystems.

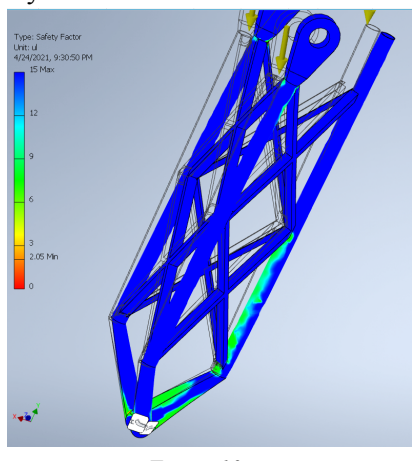


Figure 10 FEA Landing Legs

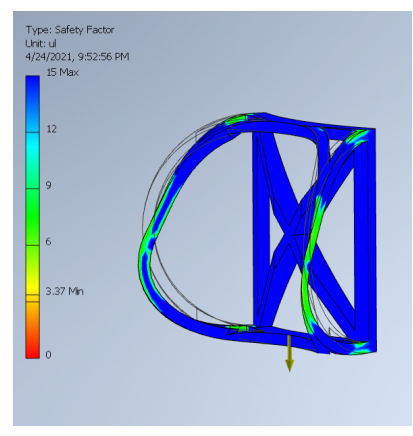


Figure 11 FEA Tank Mount

#### **MAV Design**

The JCAV is a single stage design, consisting of a landing structure, crew cabin, propellant tanks, and solar panels (in the surface configuration).

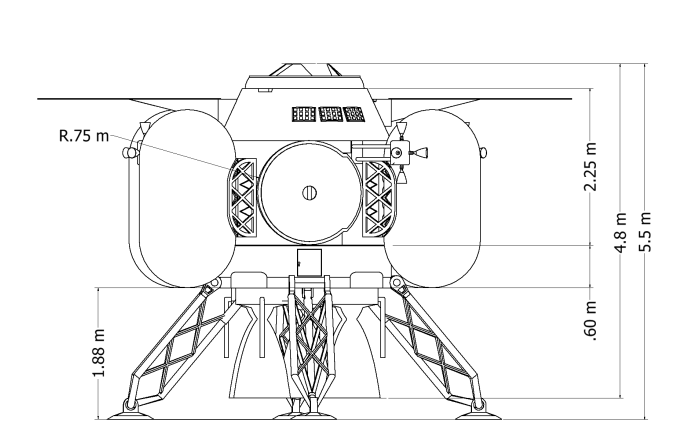


Figure 12
Landed Configuration



Figure 13
Orbital Configuration

The JCAV, upon launch, will drop the deployed solar panels and surface communications systems, along with the landing structures. The MAV is sized to fit within an SLS rocket configuration, with a total launch configuration width of about 5 m.



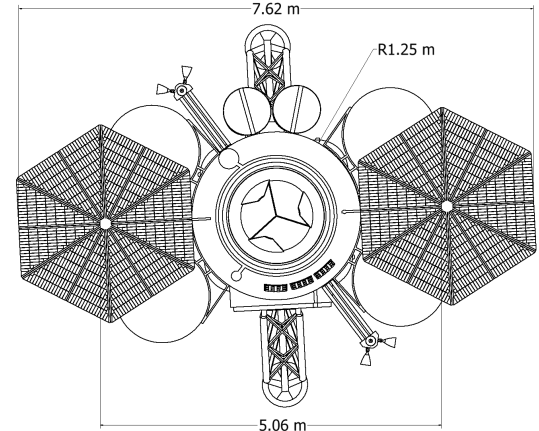
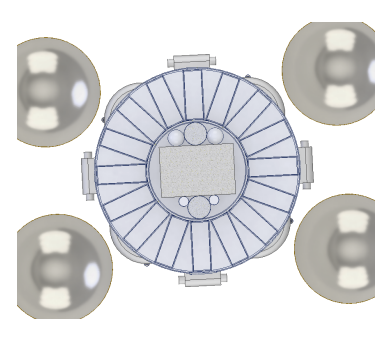


Figure 14
Dimension Views of top and side of JCAV



The sample storage system, although a simple concept, provides the JCAV with versatility in regards to storing samples. The sample storage system is a rotating, compartmentalized, section under the crew cabin of the MAV. In total, it houses 16, hermetically sealed containers, each with a volume of 0.037  $\text{m}^3$ , for a total storage volume of 0.59  $\text{m}^3$ . This considerable amount of space allows the MAV to accommodate a large range of samples and cargo.

Figure 15
Slice view of the sample storage system

The sample storage system allows for a flexible storage architecture. The entire sample storage is separately sealed and pressurized from the crew cabin. Therefore, samples can be stored from the Martian atmosphere. Anytime during the 30 day mission on mars, the crew may access the sample storage hatch (located under the crew side hatch) and can place samples in the containers as needed. Before launch, the

sample storage system will also be pressurized by the system used for life support. Given that this system is filled via the martian atmosphere, a robust dust mitigation system is required. Forward work will be conducted on this system to provide the safest possible dust mitigation.

In orbit, and upon docking with the ERV, the crew will be able access sample containers via a sealed hatch on the floor of the MAV. From this hatch, the crew may remove the samples and transfer the containers into the ERV.

A key factor of launch activities for the JCAV is the crew ingress tunnel. The crew ingress tunnel is designed to keep the crew isolated from the Martian environment in order to enter the MAV before launch, without requiring a dedicated airlock on the JCAV. Instead, the crew will rely on the use of a pressurized rover which the crew will ride to the launch site, and will connect to the MAV via the ingress tunnel (stored in front of the side hatch). Though the use of an external rover puts extra strain on the aspects of the mission architecture outside of the MAV, current proposed mission architectures for human mars mission commonly include a pressurized rover. According to the Mars Design Reference Architecture, a pressurized rover with the ability to support 2 crew members and provide a system to perform EVA from the rover [10]. Similarly, current proposed MAV mission architectures utilize a rover mounted ingress tunnel to facilitate crew ingress [7].

The design of the crew ingress tunnel is based on a few assumptions. Besides the need for a pressurized rover, this rover must also be equipped with a 1 m by 1 m square docking port, which is the specification given for a crew ingress architecture [11]. Similarly, the rover must be able to physically interface with the ingress tunnel.

The crew ingress tunnel is stored in-front of the side hatch of the MAV, and is covered by a cap which can be removed by the crew. When operations begin for the tunnel ingress, the crew will be required to perform EVA and remove the cap storing the ingress tunnel. After this is completed, the MAV will begin pressurizing the tunnel (which is sealed on the rover end) with the same system used for the crew cabin pressurization. This partial pressurization will allow the crew to easily maneuver the tunnel off the MAV and onto the docking port on the rover. At this point, after leak checks have been conducted, the crew can fully pressurize the tunnel via the rover's pressurization system. Upon full pressurization, the crew may begin operations to enter the MAV. To enter the MAV, the crew will don clean IVA suits, and travel through the ingress tunnel to the MAV side hatch. Before opening the hatch, the MAV will have been fully pressurized, such that the pressure is slightly higher than the pressure of the rover. This pressure difference will encourage a flow of air outside of the MAV further mitigating dust and contamination. The crew ingress tunnel will stay connected until lift off. Close to liftoff, the tunnel will be pyrotechnically ejected. Although the ingress tunnel is only single use, it will be removed at the latest possible event before lift-off in order to mitigate this risk.

The ingress tunnel mass and general design is based on study conducted to evaluate various MAV tunnel concepts. The JCAV ingress tunnel utilizes the collapsible tunnel concept, in order to save space and mass. Additionally, the ingress tunnel in JCAV's mission architecture is installed by the crew through mars surface EVA, removing the need for an automated alignment and connection system. In total, the estimated mass of the crew is 120 kg [11]. This mass includes the tunnel material, support structures, docking interfaces, handrails, and maintenance kit.

#### **Engine Configuration**

The MAV will consist of a single stage to orbit (SSTO) main propulsion system (MPS) with a reaction control system (RCS) for small orbital maneuvers. The engine design in the MPS will be custom built, henceforth referred to as the Mars Ascent Vehicle Engine (MAVE), as shown in Figure 15. The MAVE will utilize turbopumps in a fuel rich open cycle to allow for high efficiency. The MAVE will be regeneratively cooled using MMH [12]. The dimensions and performance parameters of the MAVE, calculated assuming 95% efficiency from Rocket Propulsion Analysis (RPA) software, are shown in Table 4 and 5 [13].

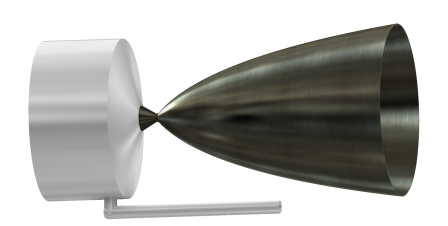
The MPS contains five 20 kN MAVE's that can be gimbaled plus or minus eight degrees in the pitch and yaw axes, four nested Aluminum-Lithium 2195 tanks that each hold oxidizer and fuel (mass per tank listed in Table 6), and a helium pressurization subsystem [14][15][16][17][13]. This subsystem will be contained within the propellant tanks, in order to address structural MAV design constraints [18]. The nested tank design was chosen to reduce volume allocation and to ensure a balanced center of mass [18]. After the MPS is depleted of fuel, the crew cabin, RCS, and nested RCS propellant tanks (mass per tank listed in Table 6) remain. There are four RCS units on the corners of the MAV that each contain four thrusters, for a total of 16 thrusters. The RCS is an innovative design utilizing the same propellant as the main engines, MON-25/MMH, using a pressure fed design [19]. Tank dimensions are shown in Table 6 which includes anti-slosh, anti-vortex, and ullage accommodations [20][21][22]. Volumes were calculated using the density of both MMH and MON-25 at 25 °C, as this is the temperature at which the propellants will be loaded on the pad.[23]

Performance Parameter	Value	Performance Parameter	Value
Delta V (MAVE) [m/s]	4893.45	RCS Propellant Mass [kg]	293.74
Delta V (RCS) [m/s]	197.80	Total Propellant Mass [kg]	15000
Required Delta V [m/s]	3791.94	Chamber Pressure [psi]	1100
Margin of Error [%]	34.52	Helium Tank Pressure [psi]	10000
Safety Factor	1.497	Maximum G-Force [g's]	2.17
MAVE Propellant Mass [kg]	14706.26	MAVE Burn Time [s]	480.78

Table 3. Summary of chemical propulsion system parameters

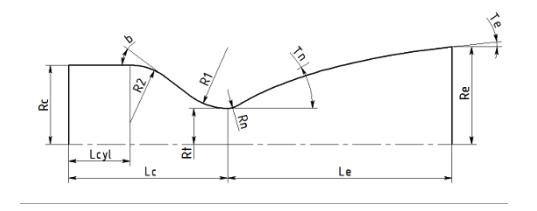
Engine Dimensions	Magnitude
Chamber Radius [mm]	65.30
Chamber Length [mm]	36.03
Throat Radius [mm]	21.56
Exit Radius [mm]	431.06
Expansion Ratio	400:1
Bell Length [mm]	1229.83
Exit Angle [degrees]	8.00

Table 4. Summary of MAVE specifications from RPA



Engine Parameter	Magnitude
Chamber Thrust [kN]	20.35
Specific Impulse at Ground [s]	326.63
Specific Impulse in Vacuum [s]	333.94
Total mass flow rate [kg/s]	5.90
Oxidizer mass flow rate [kg/s]	4.09
Fuel mass flow rate [kg/s]	1.81
Oxidizer:Fuel Ratio	2.16
Total engine mass [kg]	70
Divergence Efficiency [%]	98.90
Drag Efficiency [%]	99.16
Thrust coefficient in vacuum	2.02

Table 5. Summary of MAVE dimensions from RPA



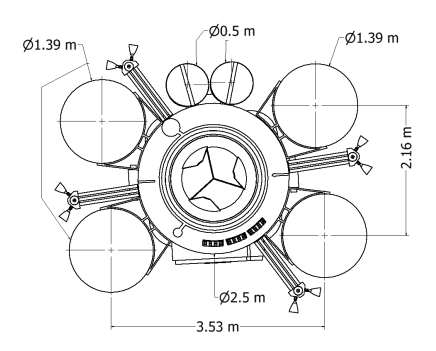


Figure 17: Top view of MAVE featuring MPS, featuring RCS tank diameters, and tank distancing

Figure 18: Side view of the MAVE RCS propellant tanks including tank height

Tank Parameters	MPS	RCS
No. Nested Tanks	4	4
Tank Volume [m³]	3.15	0.0621
Tank Mass [kg]	154	13.4
MON-25 Tank Volume [m³]	1.82	0.0379
MMH Tank Volume [m³]	1.33	0.0241
MON-25 Ullage [%]	3.49	3.49
MMH Ullage [%]	2.48	2.48
MON-25 Tank Pressure [psi]	10-50	176-333
MMH Tank Pressure [psi]	10-50	176-333

Table 6: Propellant tank design summary [24]

#### **Propellant Selection**

The MAV will utilize an innovative MON-25/MMH hypergolic propellant combination in both the main engines and the RCS. This facilitates a design that requires less complexity and power requirements than current MAV propulsion systems and allows for operations over a wide range of temperatures [25]. The inherent risk of using hypergolics in close proximity is accounted for with the Aluminum-Lithium 2195 nested tank material [26][27]. Oxidizer MON-25 is a mixture of 75% nitrogen tetroxide, N2O4, and 25% nitric oxide, NO, in mass [14]. This ratio is desirable because of its low freezing point (-55 °C) compared to traditional N2O4 oxidizers, and a freezing point similar to MMH (-53 °C) [14]. Such temperatures are important for withstanding the harsh Martian climate and allowing for less complexity than that of cryogenic propellants such as common liquid

oxygen/liquid methane designs. An ideal temperature range above -40 °C is pursued because N2O4 begins to crystallize out of MON-25 at this temperature [14]. Below 0 °C, MMH has a significant increase in viscosity as temperature decreases [14]. As a result, the constant internal tank temperature is held at 0 °C to minimize the difference in viscosity between oxidizer and fuel and optimize power consumption through heating. Minimizing viscosity difference is preferable in design of the fuel injectors. To perform the requisite temperature adjustments, the MAV will use a resistance-based patch heating system applied on the inner layer of the insulation on the propellant tanks, functioning at near 100% efficiency [28].

To date, there has not been in-space flight testing using these propellants as the MPS. However, such an engine will be designed and manufactured for use on the MAV by Agile Space Propulsion, who have evidence of manufacturing engines to TRL8 in as little as twelve months [29]. An existing N2O4/MMH engine can be retrofitted to utilize different propellants to expedite this process, and in this case, MON-25 will replace N2O4 [30]. In addition, the benefits of MON25/MMH allow for the MAV to land on Mars fully-fueled without the need for an In-Situ Resource Utilization (ISRU) system, which would create

additional timeline and design complications while increasing the possibility of a critical system failure [31][32].

#### **Thermal Information**

The Martian surface at the landing site is subject to temperature fluctuations and complications that, if not accounted for, could cause issues including freezing propellant, crystallization, and viscosity variations for the MON25/MMH fuel and oxidizer combination supplemented by NO [14].

In order to prevent these issues, the fuel tanks have been insulated with a Multi-Environment Multi-Layer Insulation (MEMLI) [33]. The fuel tanks' temperature will remain at or above 0 °C, which minimizes the variations in viscosity and prevents freezing and crystallization[14]. The configuration of MEMLI has a heat flux of 1 W/m², with an emissivity of 0.01 and a mass of 1.2 kg/m² [34]. MEMLI will be at TRL 6 [34]. The performance of MEMLI is shown at various internal and external environmental temperature differences in Table 7. The internal temperature of the propellant tanks will be kept at 0°C (to ensure no crystallization of propellant). Considering the external environmental temperature is -55°C, the average heat flux of MEMLI will be 0.96 W/m².

Temperature difference (°C)	Heat Flux (W/m²)	
20	0.35	
55	0.96	
150	2.625	

Table 7. MLI insulation heat flux at internal and external temperature differences

Polyimide, etched foil patch heaters with a single aluminum side for heat spread, will be used to heat the cabin and propellant tanks. [28]. For each propellant tank, heaters are evenly spaced patches that are 24 mm by 165 mm. Each MPS tank has 676 patches of heaters, and each RCS tank will have 52 heaters. In addition, every other heater will be inactive and will be used as a backup or in case of failure/degradation. Each heater will provide 1 W/m² of heat, and the bonding adhesive will be Stycast 2850 [28]. The

heaters perform better than the Kapton film heaters traditionally used for heating purposes in spaceflight, have a negligible change in resistance after 24 hour cycles (and less than 1% after a simulated 1033 day/night cycles simulating a Martian summer and winter), and can start at cold temperatures of down to -80 °C [28].



Figure 19. The dimensions of the heater configuration

#### **Propulsion System Changes**

The proposed propulsion system utilized staging maneuvers which was moved away from for design simplicity. Transitioned from heritage systems as Mars is a foreign environment and systems would need to be qualified for a mission there. Propellant will no longer be stored at -20 °C for further viscosity optimization. Replaced immersion heaters with patch heaters for tank simplicity. MAVE was changed from pressure fed to gas generator cycle for increased efficiency.

#### **Human Factors**

The MAV will consist of 2 astronauts with each weighing between 50 kg minimum to 98.5 kg maximum. The height range minimum and maximums will be anything between 149.5 cm to 190.5 cm. The selected suit for astronauts for the MAV flight is the IVA (Intra Vehicular Activity) with a mass of around 15 kg per suit. This will ensure the safety of the crew of 2 astronauts during launch and flight. Since the duration of the mission is rather short, an IVA suit would be suitable as it will provide comfort during the mission that is not motion intensive.

The MAV will be using two recumbent seating arrangements (approximately 25 kg each) that will give the crew capability to move freely in the seats. For crew safety, the crew will be seated perpendicular to

the direction of motion during the flight, such that most forces travel through their chest. This means that crew seats will be horizontal relative to the surface. Although this may pose some challenges to entering the MAV, the mobility of the IVA suits should allow the crew to manage the seating arrangements.

To maintain a safe environment for the astronauts, the MAV respiration environment for astronauts will consist of  $N_2$  &  $O_2$  gas tanks that will supply the crew for the mission. Estimatedly, the crew will need about 0.85 kg of oxygen per day [35]. The estimated mass for the  $N_2$  tank is 22.84 kg and the estimated mass for the  $O_2$  tank is 6.85 kg. The MAV will be supplied with 1 of each. According to performed calculations, this amount will supply the crew for 1 and a half days. This value is notably larger than the maximum flight time, but was chosen in order to provide ample air supply for the launch operations and tunnel pressurization. Accordingly, the pressure maintained inside the cabin will be maintained at 1 standard atmosphere (14.7 psi) [36].

To keep astronauts comfortable inside the MAV, a thermal system has been devised to keep the internal cabin temperature regulated. There are two parts to the system, active and passive. Both systems are similar yet slightly different to those found on the International Space Station. The active system involves using resistance-based heating patches that have been calculated to need about 355Wh to run. These patches will be attached specifically to the cabin walls, as it allows for better heat transfer. The location of the patches will not harm any electronics or the astronauts, but it is worth noting that the patches should not be touched due to them being used as a major heat source. As a result of the power consumption required to run the system, it will mainly be active when the astronauts are not in the MAV and when temperatures fall below -20 °C. This allows for the electronics and other equipment to remain functional at a safe temperature as it isn't designed to be exposed to the freezing temperatures on Mars. It will also help keep the cabin's electronics and necessary systems working and allow the astronauts to access at a reasonable temperature.

At this point, the heaters will be used to increase the temperature to a more comfortable temperature. The passive system then utilizes itself and expels heat from the astronauts and electronics to keep the cabin comfortable. The passive system in question does not use any external power or have moving parts. The major equipment associated with the passive system is multi-layered insulation (MLI) that is coated outside the cabin. These MLI layers are typically made up of Mylar and Kapton and are similar in design to what is being used on the MAV fuel tanks. The layers help to keep heat inside the cabin while also keeping external heat from entering the cabin. Thus, it allows for the cabin to stay at a comfortable temperature without getting too warm due to external factors. The MLI also helps protect astronauts inside the MAV from solar radiation [37]. The reason the MLI is coated on the outside is because of how the layers need to be set up. It requires one side that is reflective and opaque, and another side that is not reflective in order for the MLI to fully function. This helps dissipate and reflect any radiation or external heat. In addition, the reason for multiple layers of insulation is because each additional layer of insulation helps to reduce heat transfer and offer better reflection toward any radiation trying to penetrate the cabin (thermal, solar, cosmic rays).

In the event the cabin gets too warm, due to any variety of factors, a heat rejection system is built into the MAV. The heat rejection system works by maintaining a system of fans and liquid loops to transfer heat from the cabin to the external environment. These fans within the cabin ensure that air is being circulated. The air then transfers heat to a loop of water circulating throughout the cabin which then transfers the heat to a loop of allyl alcohol located outside of the cabin through a heat exchanger. The allyl loop then transfers energy to the external environment through a heat sink. The purpose of using allyl alcohol is due to the fact that it has a low freezing point of -129 degrees celsius (below the environmentally predicted temperature) [38][39]. Using allyl alcohol also requires a few safety precautions due to the highly toxic nature of the compound. Firstly, the alcohol is separated from the cabin through the usage of the water loop and secondly will be piped in a stainless steel 316L pipe to ensure compliance with safety standards [40]. In addition, the water loop will also be similarly piped, and both loops will be powered by 1/12 hp magnetic drive pumps [41]. The fans used to be IMV fans as similarly found in the International Space Station [42].

To keep the crew safe, a dust-mitigation filtration system is implemented inside the cabin that will ensure the safety of the astronauts. This is a 30 cm x 10 cm system with a mass of roughly 2-3 kg which would prevent dust from getting inside the cabin. To further ensure the cabin from exposure of any dust the crew will change into IVA suits which will prevent atmospheric dust from getting inside the cabin. Due to the brevity of the MAV mission, complex CO<sub>2</sub> scrubbing systems can be avoided. Instead, utilizing a chemical reaction with LiOH, which will react with CO<sub>2</sub> from the air effectively scrubbing it. The only requirement for full functionality is consistent airflow across the cabin. One cartridge (7 kg) of LiOH used on the Space Shuttle would be sufficient for the two astronauts [35].

For fire protection and safety of the crew, there will be a system of accessible and low powered sensors capable of detecting multiple fire signature signals and other hazardous odors and deploying a fire elimination system. Optimization will be done to fit the spacecraft environment with measured sensitivity and false alarm amelioration. There will be a total of 2 smoke detection sensors with a total mass of 6 kg that will be mounted inside the MAV. The fire elimination system will consist of a water-based foam at least [43].

The JCAV mission time will be a minimum of 5.644 hours and a maximum of 9.701 hours. To ensure the comfort of the crew the MAV will be supplied with 1 day supply of water for drinking (1.6 kg per person per day), water in food (1.15 kg per person per day) and solid foods (0.62 kg per person per day) for consumption . The food packaging will be low mass and high barrier that will be easily processed as waste. Since the mission time is short, for crew waste management system, the crew will be provided with Maximum Absorbency Garment (MAG) - an undergarment worn under IVA suit that will support the crew for up to 8 to 10 hours.

Based on the research regarding "Recommended Crew Systems Capabilities for a Mars Ascent Vehicle as a Function of Flight Duration" since the mission will not exceed 10 hours, extended waste management systems (toilets) will not be included in the MAV [44]. There are steps that NASA requires all MAV flights to contain. NASA-STD-3001 requires all MAV flights to contain space for crew for a good quality rest (even for short MAV flights), crew to perform personal hygiene and some level of medical care. To ensure that, MAV will be provided with a first aid kit and hygiene kit (no rinse shampoo, no rinse body bath, deodorant, floss, toothpaste, toothbrush) both estimating around 1.8 kg per crew for both kits [45] [44].

### Power, Avionics, & Communications (PAC) Systems

#### **JCAV Mission Modes** Surface Attempt 1 Attempt 2 Attempt 3 (9.4hrs.) (5.7hrs.) Sleep / Operations Vehicle Element Mass (kg) Daytime (Wh) ent/Orbita ent/Orbita ent/Orbita (Wh) (Wh) 354.2 272.8 449.9 Propulsion- Thermals & Sensors 20.2 792.2 Propulsion- Gimbals 36.3 0.0 2.0 0.0 2,664.0 3,384.0 2,052.0 Crew Operations, Life Support Systems, Cabin Essentials 9,035.8 200.0 5,102.4 7,649.2 10,667.1 Power Electronics & Supporting 120.0 2,940.0 1.396.5 1,813.0 2.303.0 2.940.0 Elements Communications- Surface Operations 36.8 592.0 0.0 0.0 0.0 Communications- Orbital 830.0 67.0 9426.6 11953.5 Totals: 509.9 14697.0 17802.0 9839.6

Figure 20: JCAV Power Budget- Gives breakdown of power used during different points of the mission.

JCAV utilizes two 1323.1 watt solar arrays with gallium arsenide triple-junction technology. Such has been utilized on the InSight Mars Lander as well as the proposed Orion Crewed Exploration Vehicle [46][47]. With approximately twelve hours of sunlight on Mars, the total power generated is approximately 31,754 kWh. As seen in Fig. 19, a sol on Mars (twelve hours for daytime, twelve hours for night), the JCAV consumes upwards of 20kWh, with built-in margins for emergencies. JCAV utilizes five 120V/55Ah Li-Ion batteries for storage totaling 33 kWh [48][49]. It is important to note that one of these five batteries is an extra for emergency activation if necessary. While designed for Orion, this battery

technology has been rigorously tested through the years [48] and includes a ruggedized enclosure. There is also a Power Management & Diversified Bus Unit (PMDBU) which regulates, distributes (DC-DC converters) necessary loads, and features plugins for various bus-line operations (standard 120V, 28V, 5V, 52V). Other electronics and the supporting elements accounted for include the docking sensors, docking camera, star trackers, data loggers, protection circuitry (watchdog timers, etc.), crew cabin thermals, and crew cabin sensors (pressure, temperature, environmental) [50].

JCAV features a modified FMZ-2000 flight management system from Honeywell [51-54]. There are also interactive screens aboard for the crew to utilize and adjust cabin settings as necessary. This will have been flight-proven through voyages on Orion. The main system has three glass screens with a back-facing redundant set.

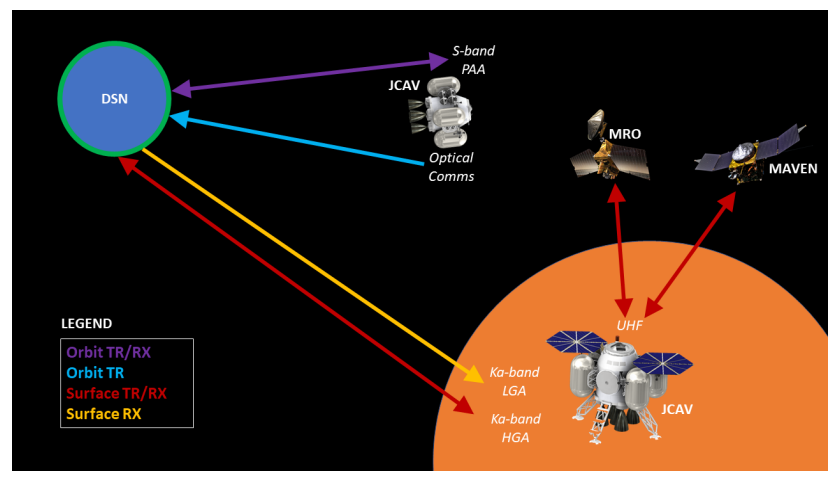


Figure 21: Communications Map- displays the available communications links

JCAV will be utilizing multiple avenues of communication including S-band [55], Ka-band [56-58], and UHF [59-60]. A Ka-band High Gain Antenna (HGA), a Ka-band Low-Gain Antenna, and a UHF antenna will all serve as the eyes and ears for NASA back on Earth during the surface stay. The Ka-band HGA is an innovative proposed design for a future Europa lander [61-62], while the LGA and UHF antenna are optimized versions of the respective antennas found on previous martian rovers including the most recent, Perseverance. As seen in Fig. 21, JCAV will use its UHF to transmit daily status telemetry to one of the orbiting Mars Relay satellites (MAVEN [63-66], MRO [67-68]) which will in turn transmit to the Deep Space Network (DSN) back on Earth. The Ka-band HGA will utilize a traveling wave tube amplifier (TWTA) and transmit and receive telemetry/commands to and from Earth [69]. The LGA will accept any incoming signals. For launch and orbital operations, conformal Haigh-Farr/Ball Aerospace phased array antennas (PAAs) [70-73], as well as an experimental optical communications payload, will be utilized. Haigh-Farr has legacy on the following: SpaceX's Dragon vehicle, commercial jets, satellites, and military vehicles requiring SATCOM, while Ball Aerospace has already delivered its PAAs designed for Orion. JCAV will utilize the conformal PAA's for direct communications to the DSN. Since it is the worry of some at NASA that the current relay system might not be sufficient in the next decade, the experimental MAScOT Optical Terminal payload will aim to demonstrate relay communications with a future orbiter and/or direct communication downlinked to Earth [74-76]. While there are some innovations being made within JCAV's communications, the systems are robust and flight-proven/will be flight proven upon JCAV's use of them.

#### **Development Timeline and Cost Estimate**

With 2025 being the starting point of the funding and development of the mission, the team would effectively have a grand total of

Total Cost Estimate (-10%)	Total Cost Estimate	Total Cost Estimate (+15%)
\$10,607,196,054	\$11,786,773,394	\$13,554,639,403

Table 8: The estimates for total mission cost, as well as the cost margin.

18 billion dollars to utilize after the collective two billion dollars per year. Using a class four AACE estimation model [77], as well as a cost estimate range of -10% to +15% [78], this provides a total mission cost estimate as seen in Table 8. A more detailed breakdown of the cost estimate can be found in Table 9, where the prices are broken down into the 2025 cost estimate and the 2033 cost estimate, using an inflation factor estimate of 2.5% per year.

The development timeline, Figure 21, takes into account the lowest TRL items first, allowing the teams at each station to devote efforts to maturing these items at a faster rate than those that are already at a higher TRL level. This also incorporates the major review requirements done in order to verify the proposal and development meet NASA's standards for a vehicle in development.

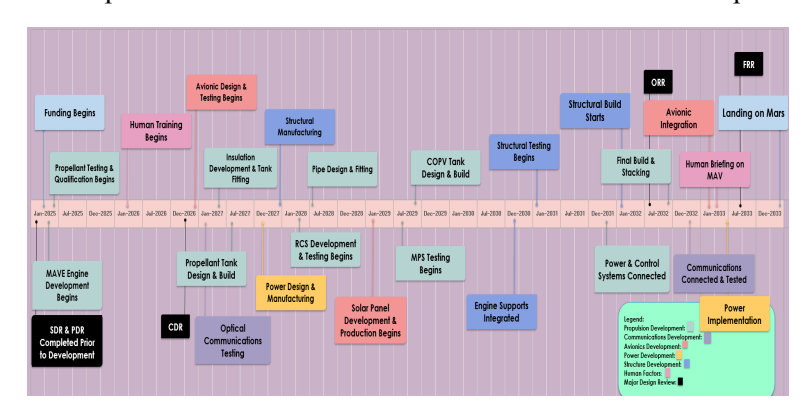


Figure 22: Development timeline for JCAV Vehicle

## Risk Analysis & TRL

#### Risk List

1 - Dust Storm	8 - Inadequate Delta-V
2 - Dust Accumulation on Solar Panels	9 - Missed Rendezvous with ERV
3 - Missed Launch Window	10 - Docking Failure
4 - MAV Legs Detachment Failure	11 - Cabin Pressure Leak
5 - Unintended Fuel/Oxidizer Mixture	12 - Communications Failure
6 - Propellant Heater Failure	13 - Sensor Malfunction
7 - Gimballing Electronic Failure	

Likelihood					
Sure		[2]			
Likely					
Possible					
Improbable	[3]	[9]	[6][13]	[7]	[1]
Unlikely			[11][12]	[10]	[4][5][8]
Consequence	Low	Slight	Moderate	High	Severe

Table 10: Risk Analysis Matrix & list

Item	Current Cost Estimate (millions)	Future Cost Estimate (2033 millions)
MAVE Engine Development [79]	\$449	\$496
RCS Engine Development [79]	\$182	\$193
Engine Propellant Qualification Testing [80]	\$20	\$23
Miscellaneous Propulsion Costs [30] [81]	\$95	\$118
Life Support Systems [82]	\$135	\$168
Astronaut IVA Suits [83]	\$0.54	\$0.67
Materials Development [81]	\$3,625	\$4,159
Structure Integration and Production [81]	\$1,087	\$1,358
Structure Testing [84]	\$815	\$1,018
Control Systems [81]	\$580	\$725
Power Internals [81]	\$118	\$147
Communications [81]	\$315	\$394
Solar Panels [81]	\$210	\$262
Human Training [85]	\$240	\$300
Ground Processing and Integration [81]	\$1,065	\$1,330
SLS Block 1B Launch Cost [86]	\$876	\$1,094

Table 9: Budget Breakdown

Subsystem	TRL
MAVE	3
RCS	3
MEMLI	6
MON25/MMH	5
Egress Tunnel	4
Sample Storage	3
Dust Mitigation	5
IVA Suits	9

Table 11: Technology Readiness Levels



## **Quad Chart**



# VUDURU M.A.E. Jemison Crewed Ascent Vehicle (JCAV) Villanova x Drexel x Rutgers



#### **Theme: Minimum Mars Ascent Vehicle**

- Deliver a Crew of 2 from Surface of Mars to Earth Return Vehicle
- Wet Mass limit of 20,000 kg
- Dry Mass limit of 5,000 kg

## Image depicting concept:



#### Innovations:

- · Utilizing an innovative engine
  - 3 engine configurations
- · Introducing an innovative fuel system
  - MON25 + MMH, Unused in Space Travel
- · Innovation of crew ingress system
  - Tunnel on Mars
  - Smooth, Problem-Free Crew Entry
- · Improved communications
  - · Deep Space Communications Payload
  - Enhances Communication Between Earth And Mars

## **Concept Synopsis:**

Our innovative idea is to further advance rocketry through use of a mixture of MON25 and MMH as propellant. Furthermore, our designed MAV features a tunnel ingress system and an experimental communications payload; some of the most cutting-edge technology used in space travel. The parts of the Jemison Crew Ascent Vehicle combine into an unparalleled method of leaving the Red Planet..

## **Appendix**

## **Calculations**

ROCKET EQUATION:  $\Delta u = Isp * g_0 * ln(\frac{m_f}{m_i})$ 

 $\Delta u$  - change in velocity

Isp - Specific impulse of rocket engine

 $g_0$ - standard acceleration due to gravity, 9. 807  $\frac{m}{s^2}$ 

 $m_f$ - final mass

 $m_i$ - initial mass

GRAVITY LOSS:  $\Delta V_{GL} = g_m t_b sin(\phi)$ 

 $g_m$ - standard acceleration due to gravity on Mars,  $3.71 \frac{m}{s^2}$ 

 $t_h$ - duration of burn time

φ- flight path angle at burnout

BENEFIT OF MARS TANGENTIAL VELOCITY:  $V_{MH} = \omega_{M} r \cos \lambda \cos (in cang)$ 

[MarsBenefit]

 $\omega_{M}$ - rotational velocity of Mars

 $r_{\scriptscriptstyle M}$ - radius of Mars

 $\lambda$  - latitude at take off

incang - inclination angle of the orbit

STAGE BURN TIME CALC:  $\Delta t = (M * m_o) * (1 - e^{-(\Delta V/V_e)})$ 

M - mass of rocket at start of stage

 $m_o$  - mass flow rate

 $\Delta V$ - delta V of burn

 $V_{\rho}$ - exhaust velocity

ANTI SLOSH CALCULATIONS:  $s \le 0.2 R$ ,  $\alpha = (2 w/R) - (w^2/R^2)$ 

s - spacing between baffles

R - radius of tank

 $\alpha$  - fraction of the tank cross-sectional area covered by the baffle

w - width of baffle

LIFE SUPPORT COST ESTIMATES:

$$Cost = 5.65 * 10^{-4} * Q^{0.59} * M^{0.66} * 80.6^{S} * (3.81 * 10^{-55})^{(1/(IOC - 1900))} * B^{-0.36} * 1.57^{D}$$

Q- total quantity of materials

*M*- dry mass of materials (kg)

S- mission specification

*IOC*- year of initial operational capacity (2033)

B- hardware generation

D- estimated difficulty

BUDGET CALC FOR GENERAL MATERIALS:

$$Cost = a * Q^b * W^c * d^S * e^{(1/(IOC-1900))} * B^f * g^D * inflation$$

$$a - 9.51 * 10^{-4}$$

Q- total quantity

b-0.59

W- dry mass (kg)

c- 0.66

d-80.6

S- system type

$$e$$
- 3.81 \* 10<sup>-55</sup>

$$f - 0.36$$

*g*- 1.57

D- difficulty

*inflation*- the inflation rate (assumed here to be 2.5)

## **ORBITAL EQUATIONS:**

Kepler's Third Law:  $T^2/R^3 = (4*\pi^2)/(G*M)$  - Used for calculating orbital period

T = time in seconds

R = orbital radius

G = gravitational constant = 6.67 \*  $10^{-11}m^3/(kg * s^2)$ 

M = Mass of Mars in kg

Vis- Viva Equation:  $v = \sqrt{(\mu((1/r) - (1/a)))}$  - Used for Hohmann Transfer Calculations

v =velocity

 $\mu$  = Standard Gravitational Parameter of Mars

r = orbital radius

a = length of semi-major axis

Orbital Velocity:  $v = \sqrt{(GM)/R}$ 

G = gravitational constant

M = mass of Mars

R = orbital radius

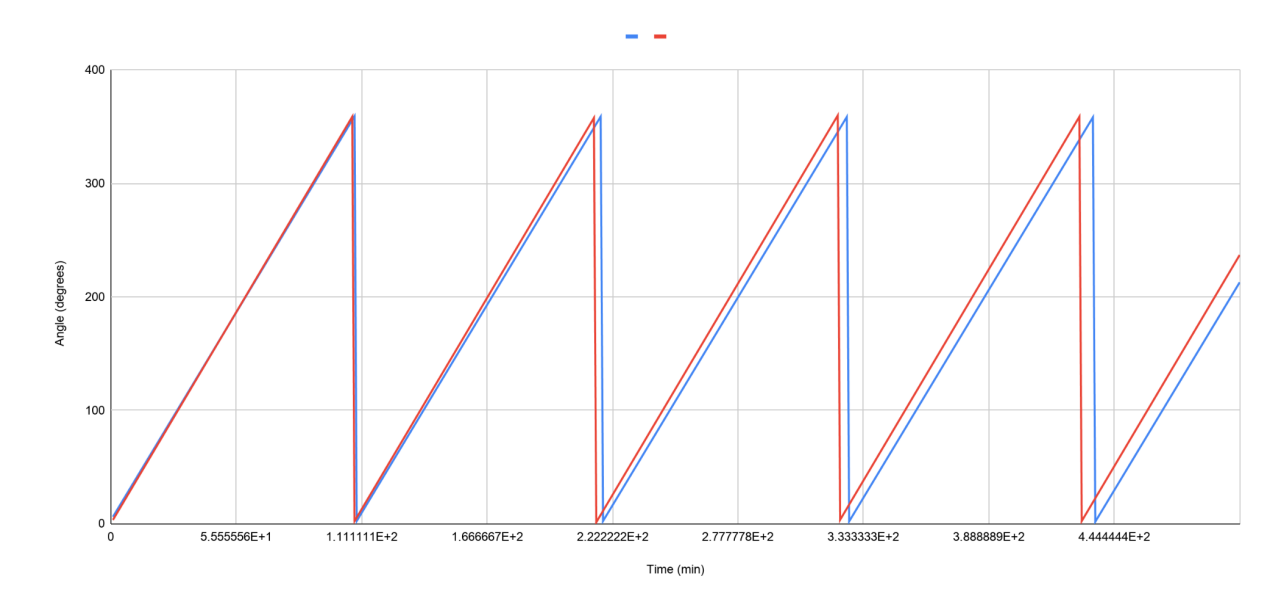
Equations Used for Simulating Times: - Timing and Launch Window Calculation:

ERV angular velocity: 360 degrees/ 109.05 min = 3.30 degrees / min.

ERV orbit :  $x(t) = 3.30t + 2.79 \leftarrow initial starting angle of ERV$ 

Hohmann Transfer orbit: y(t) = 3.35t,  $3.35 \text{ degrees/min} \leftarrow \text{angular speed of MAV on transfer orbit}$ 

2 equations above were run on MATLAB for 500 seconds. Data set was imported into Excel



The red line represents the MAVs path and the blue line represents the ERV path.

#### References

- [1] J. Hickman, A. Wilhite, D. Stanley, D.R. Komar. "Optimization of the Mars Ascent Vehicle for Human Space Exploration. Journal of Spacecraft and Rockets," Journal of Spacecraft and Rockets. p. 361-370.
- [2] Hohmann Transfer, ai-solutions.com/ freeflyeruniversityguide/hohmann transfer.htm.
- [3] "Human Landing Sites Study (HLS2) Newsletter," *NASA*. [Online]. Available: https://www.nasa.gov/sites/default/files/atoms/files/hls2\_newsletter\_02-19\_v19.pdf
- [4] Hop David, "Cosmic Train Schedule," [Online]. Available: http://clowder.net/hop/railroad/sched.html
- [5] "Cosmic Materials Space Research Group," *Eötvös University / Hungarian Academy of Sciences*. [Online]. Available: http://planetologia.elte.hu/indexe.html
- [6] "Welcome to the JMARS Website." *JMARS*. [Online]. Available: jmars.asu.edu/
- [7] T. P. Polsgrove, T. K. Percy, and M. Rucker, "Update to Mars Ascent Vehicle Design for Human Exploration," *National Aeronautical and Space Association*. [Online]. Available: https://ntrs.nasa.gov/api/citations/20190001229/downloads/20190001229.pdf.
- [8] Vicente-Retortillo, Á., Martínez, G.M., Renno, N. *et al.* Seasonal Deposition and Lifting of Dust on Mars as Observed by the Curiosity Rover. *Sci Rep* 8, 17576 (2018). https://doi.org/10.1038/s41598-018-35946-8
- [9] A. Guinness, Edward, E. Leff, Craig, E. Arvidson, Raymond. "Two Mars Years of Surface Changes Seen at the Viking Landing Sites," *Department of Earth and Planetary Sciences and McDonnell Center for the Space Sciences, Washington University. Journal of Geophysical Research.* November 30, 1982. Available: https://agupubs.onlinelibrary.wiley.com/doi/epdf/10.1029/JB087iB12p10051
- [10] "Human Exploration of Mars Design Reference Architecture 5.0" NASA, [Online]. https://www.nasa.gov/pdf/373665main NASA-SP-2009-566.pdf
- [11] M. Rucker, et. al., "Mars Surface Tunnel Element Concept," IEEE, [Online]. https://ieeexplore.ieee.org/document/7500781
- [12] S. Shine and S. Nidhi, "Review on film cooling of liquid rocket engines," *Propulsion and*

- Power Research, vol. 7, no. 1, pp. 1–18, 2018.
- [13] L. Osborne (AGILE Space Industries) and Propulsion Team, "Overall propulsion system review," 2021
- [14] H. P. Trinh, C. Burnside, and H. Williams, "International Astronautical Congress (IAC)," in *Assessment of MON-25/MMH Propellant System for Deep-Space Engines*.
- [15] M. Wade, "ATE," *Astronautix*. [Online]. Available: http://www.astronautix.com/a/ate.html.
- [16] J. Dumoulin, "NSTS 1988 News Reference Manual.", NASA, 1988. Reference from Main Propulsion System section.
- [17] "Electromechanical Actuators," *Moog-Electromechanical Actuators-Datasheet*. [Online]. Available:https://www.moog.com/content/dam/moog/literature/Space\_Defense/spaceliterature/actuationmechanisms/Moog-Electromechanical Actuators-Datasheet.pdf. [Accessed: 26-May-2021].
- [18] T. P. Polsgrove, T. Percy, M. Rucker, H. Thomas, "Update to Mars Ascent Vehicle Design for Human Exploration," *Marshall Space Flight Center*, 2019. [Online]. Available: https://ntrs.nasa.gov/api/citations/20190001229/downloads/20190001229.pdf
- [19] J. Dumoulin, "Reaction Control System," *NASA*. [Online]. Available: https://science.ksc.nasa.gov/shuttle/technology/sts-newsref/sts-rcs.html#sts-rcs.
- [20] J. G. Perez, R. A. Parks, and D. R. Lazor, "Validation of Slosh Model Parameters and Anti-Slosh Baffle Designs of Propellant Tanks by Using Lateral Slosh Testing," *NASA Marshall Space Flight Center*. [Online]. Available: https://ntrs.nasa.gov/api/citations/20130000590/downloads/20130000590.pdf. [Accessed: 20-May-2021].
- [21] H. Yang, J. Peugeot, J. West, "A Computational Fluid Dynamics Study of Swirling Flow Reduction by Using Anti-Vortex Baffle," American Institute of Aeronautics, Marshall Flight Center. 2017.
- [22] G. Sutton, O. Biblarz, "Rocket Propulsion Elements," [Online]. Available: http://mae-nas.eng.usu.edu/MAE\_5540\_Web/propulsion\_systems/subpages/Rocket\_Propulsion\_E lements.pdf
- [23] L. Kohout, A. Colozza, "Comparison of Mars Aircraft Propulsion Systems," [Online]. Available: https://ntrs.nasa.gov/citations/20030056588
- [24] "Reaction Control Quick Reference Sheet," *Apollo News Reference*. [Online]. Available: https://www.hq.nasa.gov/alsj/LM10 Reaction Control ppRC1-12.pdf.
- [25] T. P. Polsgrove et al., "Human Mars ascent vehicle configuration and performance sensitivities," 2017 IEEE Aerospace Conference, 2017, pp. 1-15, doi: 10.1109/AERO.2017.7943583.
- [26] S. K. Borowski, "Robotic Planetary Science Missions Enabled With Small NTR Engine/Stage Technologies." *AIP Conference Proceedings*. [Online]. Available: https://ntrs.nasa.gov/api/citations/19960002568/downloads/19960002568.pdf.

- [27] "Micropump for MON-25/MMH Propulsion and Attitude Control," *SBIR*. [Online]. Available: https://www.sbir.gov/sbirsearch
- [28] G. C. Cucullu III, M. Ochoa, and J. Ruby, "Results of All Polyimide, Etched Foil Heater Qualification and Failure Limit Testing," *International Conference on Environmental Systems*, Jul. 2017.
- [29] "Agile Space Propulsion," *Agile Space Industries*. [Online]. Available: https://www.agile.space/agile-space-propulsion.
- [30] "Aerojet-General LR87 Liquid Rocket," *National Museum of the United States Air Force*, 14-Mar-2016. [Online]. Available: https://www.nationalmuseum.af.mil/ Visit/Museum-Exhibits/Fact-Sheets/Display/Article/197696/aerojet-general-lr87-liquid-rocket/.
- [31] J. Hickman, A. Wilhite, D. Stanley, D.R. Komar."Optimization of the Mars Ascent Vehicle for Human Space Exploration. Journal of Spacecraft and Rockets," *Journal of Spacecraft and Rockets*. p. 361-370.
- [32] M. Hecht, et al., "Mars Oxygen ISRU Experiment [MOXIE]," *Space Science Reviews*, vol. 217, no. 1,Jan. 2021.
- [33] S. A. Dye, A. Kopelove, "Multi-Environment MLI: Novel Multi-functional Insulation for Mars Missions," *NASA & Quest Thermal Group*. [Online]. Available: https://sbir.nasa.gov/SBIR/abstracts/17/sbir/phase1/SBIR-17-1-Z10.01-9245.html .
- [34] A. Kopelove and T. Kaleem, "MEMLI information," 2021.
- [35] "Air revitalization UMD." [Online]. Available: https://spacecraft.ssl.umd.edu/academics/697S19L16.airsystems.pdf.
- [36] Julie A. Levri, et.al., Advanced Life Support Equivalent System Mass Guidelines Document NASA TM-2003-212278, September 2003
- [37] Sbir.gov. 2021. *Multi-Environment MLI: Novel Multi-Functional Insulation for Mars Missions* | *SBIR.gov.* [online] Available at: <a href="https://www.sbir.gov/sbirsearch/detail/1426479.">https://www.sbir.gov/sbirsearch/detail/1426479.</a>>.
- [38] PubChem. 2021. *Allyl alcohol*. [online] Available at: <a href="https://pubchem.ncbi.nlm.nih.gov/compound/Allyl-alcohol#section=Boiling-Point">https://pubchem.ncbi.nlm.nih.gov/compound/Allyl-alcohol#section=Boiling-Point</a>.
- [39] *Eötvös University Cosmic Materials Space Research Group / Planetology, Planetary Science.* [Online]. Available: http://planetologia.elte.hu/indexe.html.
- [40] "Allyl Alcohol Product Safety Bulletin." Lyondellbasell.
  https://www.lyondellbasell.com/globalassets/documents/chemicals-technical-literature/allylalcohol---product-safety-bulletin---march-2019.pdf
- [41] "1/12 hp HP Polypropylene 115V Magnetic Drive Pump, 21.9 ft Max. Head," *Grainger*. [Online]. Available: https://bit.ly/3bZPGUy

- [42] D. E. Link and S. F. Balistreri, "Inter-Module Ventilation Changes to the International Space Station Vehicle to support integration of the International Docking Adapter and Commercial Crew Vehicles." NASA, Bellevue, Jul-2015.
- [43] X. Wang, H. Zhou, W. P. Arnott, M. E. Meyer, S. Taylor, H. Firouzkouhi, H. Moosmüller, J. C. Chow, and J. G. Watson, "Evaluation of gas and particle sensors for detecting spacecraft-relevant fire emissions," *Fire Safety Journal*, vol. 113, p. 102977, 2020.
- [44] R. L. Howard, "Recommended Crew Systems Capabilities for a Mars Ascent Vehicle as a Function of Flight Duration." *NASA*, *Houston*.
- [45] P. Lopez, B. Mattfeld, C. S. Binera, and K. Goodliff, "Logistics Needs for Potential Deep Space Mission Scenarios Post Asteroid Redirect Crewed Mission." *NASA*.
- [46] "Power," ESA. [Online]. Available: https://www.esa.int/Science\_Exploration/Human\_and\_Robotic\_Exploration/Orion/Power.
- [47] "InSight Lander," NASA, 21-May-2020. [Online]. Available: https://mars.nasa.gov/insight/spacecraft/about-the-lander/.
- [48] A. Buonanno, "Updates of the Next Generation Lithium-ion Space Chemistry, for improved Energy density and Improved Cycle Life," in NASA Space Battery Workshop.
- [49] "High energy, long life and low maintenance lithium-ion cell," Eaglepicher Technologies. 2020. [Online]. Available: https://www.eaglepicher.com/sites/default/files/LP%2032770.pdf
- [50] "Main Systems ISS," *NASA*. [Online]. Available: https://www.nasa.gov/pdf/167129main\_Systems.pdf
- [51] *Honeywell*, "FMZ-2000 Flight Management Systems." [Online]. Available: https://www.redimec.com.ar/contenido/productos/pdf/1425393201\_1.pdf.
- [52] O. Olofinboba, C. Hamblin, M. Dorneich, R. DeMers, J. Wise, "The Design of controls for NASA's Orion Crew Exploration Vehicle," *Proc. of the Association for Aviation Psychology* 2008 Conference. 2008.
- [53] S. Gaudin, "The Orion Spacecraft is no Smarter than Your Phone," [Online]. Available: https://www.computerworld.com/article/2855604/the-orion-spacecraft-is-no-smarter-than-your-phone.html
- [54] T. Cichan, et al. "The Orion Spacecraft as a Key Element in a Deep Space Gateway," [Online]. Available:https://www.lockheedmartin.com/content/dam/lockheed-martin/eo/photo/webt/Orion-Spacecraft-as-a-Key-Element-to-Deep-Space.pdf

- [55] *General Dynamics*, "S-Band TDRSS / Deep Space Network (DSN) Transponder," [Online]. Available:https://gdmissionsystems.com/products/communications/spaceborne-communications/tracking-telemetry-and-control/s-band-tdrss-dsn-transponder
- [56] N. Smith Kilkenny, "KA-Band Represents the Future of Space Communications," [Online]. Available: https://www.nasa.gov/mission\_pages/station/research/news/ka\_band
- [57] *Mars Reconnaissance Orbiter*, "Ka-Band Communications," [Online]. Available: https://mars.nasa.gov/mro/mission/communications/commkaband/
- [58] M. Koziol, "How NASA is Adapting to Busier and Noisier Communications with Mars," IEEE Spectrum. 2021. [Online]. Available: https://spectrum.ieee.org/tech-talk/telecom/wireless/how-nasa-is-adapting-radios-to-a-noisier-mars
- [59] "Communications," *NASA Mars 2020 Mission Perseverance Rover.* [Online]. Available: https://mars.nasa.gov/mars2020/spacecraft/rover/communications/#UHF-Antenna
- [60] "Communications with Earth," *NASA Science Mars Exploration Program*, [Online]. Available: https://mars.nasa.gov/msl/mission/communications/#radio-waves
- [61] N. Chahat, "Europa Lander 13th European Conference on Antennas and Propagation All-Metal Dual Frequency Rhcp High Gain Antenna for the Extreme Environments of a Potential Europa Lander," *Jet Propulsion Laboratory, NASA.* 2019
- [62] N. Chahat et al., "All-Metal Dual-Frequency RHCP High-Gain Antenna for a Potential Europa Lander," *IEEE Transactions on Antennas and Propagation*, vol. 66, no. 12, pp. 6791-6798, Dec. 2018.
- [63] K. Hille, "NASA's MAVEN Continues to Advance Mars Science and Telecommunications Relay Efforts," *NASA Goddard Space Flight Center*. [Online]. Available: https://www.nasa.gov/feature/goddard/2021/maven-continues-to-advance-mars-science-and-telecommunications-relay-efforts
- [64] "Space Communications with Mars," *Luxorion*. [Online]. Available: http://www.astrosurf.com/luxorion/qsl-mars-communication3.htm
- [65] "The Maven Spacecraft," *MAVEN, Mars Atmosphere and Volatile Evolution Mission*. [Online]. Available: https://lasp.colorado.edu/home/maven/about/spacecraft/
- [66] NASA, "Electra Relay Radio on MAVEN Mission to Mars," [Online]. Available: https://www.nasa.gov/jpl/maven/electra-relay-radio-pia17952/#.YLB9wqhKhPY
- [67] R. Zureck, S. Smrekar, "An overview of the Mars Reconnaissance Orbiter (MRO) science

- mission," *Journal of Geophysical Research Vol 112*. [Online]. Available: https://agupubs.onlinelibrary.wiley.com/doi/pdf/10.1029/2006JE002701
- [68] J. Taylor, D. Lee, S. Shambayati, "Mars Reconnaissance Orbiter Telecommunications," *Deep Space Communications and Navigation Systems Center of Excellence*. 2006. [Online]. Available: https://descanso.jpl.nasa.gov/DPSummary/MRO 092106.pdf
- [69] *L3 Harris* "Traveling Wave Tubes," [Online]. Available: https://www.l3harris.com/all-capabilities/traveling-wave-tubes
- [70] "Haigh-Farr, Inc.," Haigh Farr. [Online]. Available: https://www.haigh-farr.com/products/antennas/conformal.
- [71] "Wraparound Antennas," https://www.haigh-farr.com/docs/default-source/products-data-sheets/general wraparound-antennas revb.pdf?sfvrsn=4bfd8723 2.
- [72] "Commercial Phased Arrays," Mar-2020. Available: https://www.ball.com/aerospace/Aerospace/media/Aerospace/Downloads/D3359\_Commercial\_Phased Arrays\_0320.pdf?ext=.pdf
- [73] Ball Aerospace and Technologies Corp. "Ball Aerospace Delivers Orion Phased Array Antenna EDUs," [Online]. Available: http://www.spaceref.com/news/viewpr.html?pid=35478
- [74] H. Safani, "Operations of the Optical Communications Demonstration for the Orion EM-2 Mission," [Online]. Available: https://ntrs.nasa.gov/citations/20190025761
- [75] A. Seas, B. Robinson, T. Shih, F. Khatri, M. Brumfield, "Optical Communications Systems for NASA's Human Space Flight Missions," *NASA Technical Reports Server*. [Online]. Available: https://ntrs.nasa.gov/citations/20180007088
- [76] T. Jedrey, et al. "Conceptual Studies for the Next Mars Orbiter (NeMO)," in Industry Day. Available: http://images.spaceref.com/news/2016/NeMOIndustryDay.pdf
- [77] "Cost Estimate Classification System as Applied in Engineering, Procurement, and Construction for the Process Industries", *AACE International*. 2005. [Online]. Available: https://www.costengineering.eu/Downloads/articles/AACE\_CLASSIFICATION\_SYSTEM.pdf
- [78] M. Simard and D. Lewis, "Cost estimations and development timeline techniques," 2021.
- [79] E. Friedland, J. Nieroski, "Liquid Rocket Engine Cost Estimating Relationships," *Aerospace Corporation*. 1965. [Online]. Available: https://doi.org/10.2514/6.1965-533
- [80] ''Aerospace Energy Standard Prices for DOD Customers Effective 1 OCT 2017," *Defense Logistics Agency. 2017.* [Online]. Available: https://www.dla.mil/Portals/104/Documents/Energy/Standard%20Prices/Aerospace%20Prices/E\_2017Oct1AerospaceStandardPrices\_160829.pdf

- [81] R. Rolley, R. Potter, S. Zusack, S. Saikia, "Life Cycle Cost Estimation of Conceptual Human Spaceflight Architectures," *American Institute of Aeronautics and Astronautics*. 2017.
- [82] H. Jones, "The Impact of Lower Launch Cost on Space Life Support," *NASA Ames Research Center*. [Online]. Available: https://ntrs.nasa.gov/api/citations/20180007067/downloads/20180007067.pdf
- [83] "Under Pressure, The Past, Present, and Future Market for Spacesuits," Space Angels Network. 2016. [Online]. Available: https://uploads-ssl.webflow.com/5a95af2d0f177000014a2446/5af1b905cc8a1316b3020ee5\_UND ER%20PRESSURE%20-%20SPACESUIT%20MARKET%20REPORT%20-%20JULY2016%20 (online).pdf
- [84] B. Fow, K. Brancato, B. Aklire, "Guidelines and Metrics for Assessing Space System Cost Estimates," *Rand, Project Air Force*. 2008. [Online]. Available: https://www.rand.org/content/dam/rand/pubs/technical\_reports/2008/RAND\_TR418.pdf
- [85] "Astronaut Selection and Training," *NASA, Lyndon B. Johnson Space Center.* [Online]. Available: https://www.nasa.gov/centers/johnson/pdf/606877main FS-2011-11-057-JSC-astro trng.pdf
- [86] J. Foust, "Inspector General Report Warns of Cost and Schedule Problems for Europa Clipper," *Spacenews*. 2019. [Online]. Available: https://spacenews.com/inspector-general-report-warns-of-cost-and-schedule-problems-for-europa -clipper/